Small Angle Neutron Scattering from Polyelectrolyte Solutions: From Disordered to Ordered Xanthan Chain Conformation

Michel Milas, Marguerite Rinaudo, Robert Duplessix,† Redouane Borsali,* and Peter Lindner‡

Centre de Recherches sur les Macromolécules Végétales, CERMAV-CNRS, and Joseph Fourier University, BP 53, F-38041 Grenoble Cedex 9, France

Received March 18, 1994; Revised Manuscript Received February 15, 1995®

ABSTRACT: This work discusses the static properties of xanthan solutions in the semidilute concentration range as revealed by small angle neutron scattering (SANS). Samples having different molecular weights were used to investigate the scattering properties as a function of polymer concentration C_p, added salt concentration C_s, and temperature. The results show the existence of a broad peak in the investigated range of C_p and momentum transfer q. The positions of these peaks scale roughly as $C_p^{1/2}$ in the high-concentration range. As the concentration decreases, the system shows a conformational transition characterized by a decrease in the exponent. This change in the exponent is interpreted as a progressive shift from ordered to disordered conformation of xanthan for which the peak position is expected to scale with the concentration as $C_p^{1/2}$ too. The equivalent Bragg interparticle distance has been found in good agreement with hexagonal packing, assuming a single stretched chain in the low-C_p range (disordered xanthan conformation) and a double-stranded chain, at least locally, in the high C_p range (ordered conformation).

I. Introduction

Solution properties of polyelectrolytes exhibit a behavior which, in most cases, differs considerably from that of uncharged polymers. The origin of this feature comes obviously from the presence of charges along the chain and leads to intra- and intermacromolecular interactions. These interactions, if they are not screened out, by adding external salt for instance, have strong consequences on both static and dynamic properties of the system. These complex mechanisms involving interacting polyions, counterions, and co-ions have attracted many researchers, and over the past decade there has been considerable interest in the static and dynamic properties of such systems from both theoretical[1-11] and experimental points of view.[12-24] Various experimental techniques have been used to understand the behavior of such charged complex systems: small angle X-ray (SAXS) and neutron scattering (SANS), elastic and quasi elastic light scattering, and viscosity. In this paper we shall present and discuss our experimental results obtained using SANS.

The results concern xanthan which is a charged bacterial polysaccharide. Two conformations characterize this polymer and were investigated previously[25-30] using different techniques. At low polymer concentration, low salt concentration, and higher temperature, the xanthan is in its disordered conformation, i.e. a wormlike chain with a moderate persistence length (L_P ~ 50 Å); when temperature is decreased or external salt concentration is added (above 10^{-2} M at 25 °C), an ordered conformation corresponding to a helical structure with a high intrinsic persistence length (L_P ~ 350 Å, based on a monohelical structure assumption), is stabilized.[31] This conformation can be either a single helix or a double helix, as it is still under discussion.[32] Moveover, when the polyelectrolyte concentration increases and reaches a critical value, the system presents a cholesteric mesophase formation.[33]

This paper presents experimental data concerning the elastic neutron scattering intensity of xanthan solutions as a function of polymer concentration, ionic concentration, temperature, and molecular weight. The results give new information on the conformation of the xanthan chain in solution.

II. Experimental section

II.1. Small Angle Neutron Scattering. SANS experiments were performed on D11 and D17 diffractometers at the Institut Laue Langevin (ILL), Grenoble, France. The scattering wavevector $q = 4\pi \sin(\theta/2)/\lambda_0$, where θ is the scattering angle and λ_0 is the wavelength of the neutrons, ranges from 0.005 to 0.085 Å^{-1}. All the data were treated according to standard ILL procedures (correction of transmission and thickness samples) for small angle isotropic scattering. The temperature control was ±0.1 °C.

II.2. Materials. Xanthan is a polysaccharide produced by Rhone-Poulenc and purified as usual. It contains uronic acids and behaves as a polyelectrolyte characterized by a charge parameter $\lambda \simeq 1$ as described by Katchalsky *et al.*[1] for the disordered single chain conformation and an ionic content about 1.56×10^{-3} equiv/g (or 641 g/equiv).

Samples with different molecular weights were prepared by enzymic degradation from the native sample; the different molecular weights used are $M_w = 3.6 \times 10^6$, 7×10^5, and 2×10^5. All these samples were preheated before experiments.[34] The solutions of the Na salt form of xanthan were prepared by dissolution of an exact weight in D_2O. NaBr in powder form or in 1 M NaBr solution in D_2O solution was added to get the appropriate salt concentration. It is well-known that aggregates or microgels are often present in a very small amount and no modification of the main properties was observed.[35]

The conformational transition which is induced by a change of temperature or salt concentration was examined by different techniques.[35] In this work the optical rotation at 300 mm was determined by using a Fica Spectropol 1b instrument with a 0.5 cm quartz cell thermostated with a Haake thermostat.

The upper estimates of the overlap concentration C^* based on the well-known formula $C^* = M_w/(N_A 4\pi R_G^3/3)$, where R_G is the radius of gyration of the molecule and N_A the Avogadro number, is $C^* = 7 \times 10^{-4}$ g/mL. This value calculated for the lower molecular weight sample (2×10^5), assuming a wormlike chain model, indicates that all the data are obtained in the semidilute regime.

* To whom correspondence should be addressed.
† UFR de Physique, Université de Bordeaux I, Talence, France.
‡ Institut Laue Langevin BP 156, Grenoble Cedex 9, France.
® Abstract published in *Advance ACS Abstracts,* April 1, 1995.

0024-9297/95/2228-3119$09.00/0

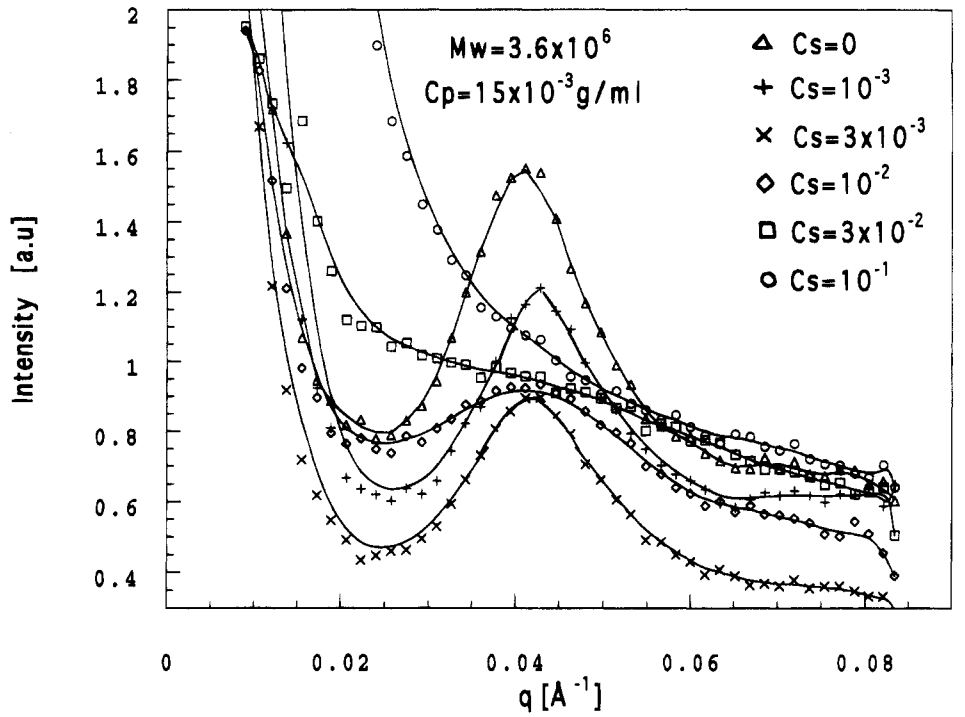

Figure 1. Effect of Added Salt Variation of $I(q)$ as a function of q for ($M_w = 3.6 \times 10^6$, $C_p = 15 \times 10^{-3}$ g/mL) xanthan at the different added salt concentrations C_s shown ($T = 25$ °C).

III. Results and Discussion

III.1. Effect of Salt Concentration. In salt-free solution ($M_w = 3.6 \times 10^6$, $Cp = 15 \times 10^{-3}$ g/mL, $T = 25$ °C) when xanthan is in the ordered conformation, a very distinct and broad peak with an upturn in the small q range is observed. Figure 1 shows the effect of added salt concentration C_s. One observes that the addition of a simple electrolyte (NaBr) decreases the peak intensity and maintains its position roughly constant. This result, also observed at higher polymer concentrations and for different molecular weights, reflects the electrostatic nature of the peak. The presence of a peak indicates a preferential interparticle distance in solution; its position must be related to this distance as discussed below.

One observes that the region $q < q_{max}$ is very sensitive to the addition of salt and that of $q > q_{max}$ preserves a level of scattering close to the value in the absence of salt, as expected by most theoretical models for electrostatic interaction in the semidilute range of concentration.

When enough salt is added, the scattering behavior is closer to that of a neutral polymer. For example this neutral type behavior is reached for $M_w = 3.6 \times 10^6$, $C_p = 15 \times 10^{-3}$ g/mL at the value of C_s above 10^{-2} M NaBr (see Figure 1) or for $C_p = 10^{-2}$ g/mL above $C_s \simeq 5 \times 10^{-3}$ M NaBr. The exact value of C_s at which the peak disappears cannot be obtained with high accuracy and only a rough estimate of the ratio C_p/C_s about 2 can be given. The value of this ratio has been already discussed.[36] The same behavior has been observed for other systems.[14]

III.2. Effect of Polymer Concentration and Molecular Weight in Salt-Free Solutions. In the last section we showed the electrostatic nature of the interactions which are at the origin of the peak. This section, however, discusses what type of conformation is involved in the absence of added salt. Figure 2 represents typical scattering intensity curves $I(q)$ as a function of the wavevector q at different polyelectrolyte concentrations in salt-free solutions. In the range of the investigated concentrations, 4×10^{-3} g/mL $< C_p < 3 \times 10^{-2}$ g/mL for $M_w = 2 \times 10^5$, a very distinct and broad peak is observed. The position of the peak maximum q_{max} is shifted toward higher q values with increasing concentration but is independent of the molecular weight. One notes that for all concentrations this peak is accompanied by an upturn of the scattered intensity for $q < 0.02$ Å^{-1}. To be more complete, in our observation, no secondary peak was detectable. The same behavior (broad peak, no secondary peak and an upturn at $q < 0.02$ Å^{-1} of $I(q)$) is observed for other samples having different molecular weights. For concentrations lower than 4×10^{-3} g/mL the peak should be at $q < 0.02$ Å^{-1}, i.e. in the upturn of the scattered intensity, and then is no more observed.

In the range of concentration investigated, the scattering vectors of the peak maxima q_{max} are plotted in Figure 3 as a function of C_p for the three studied molecular weights. One distinguishes clearly two regimes. The semidilute feature at higher concentrations is characterized by a scaling law $q_{max} \sim C_p^{1/2}$. As the concentration decreases, this behavior is lost. In fact the crossover occurs at a concentration close to $C_p = 10^{-2}$ g/mL, which is about 70 times higher than C^*. Thus this decrease of the slope cannot be explained on the

Table 1. Melting Temperature (T_M) and Temperature Range of the Conformational Transition of Xanthan as a Function of Its Concentration in Pure Water[35]

		transition range (in °C)	
$10^{-3}C_p$, g/mL	T_M, °C	from	to
1.5	12	<0	22
2.5	17.5	2.5	27.5
3.5	23	7	33
4.25	25	10	35
5	31	16	41
10	45	30	55
20	58	43	68
30	74	59	84

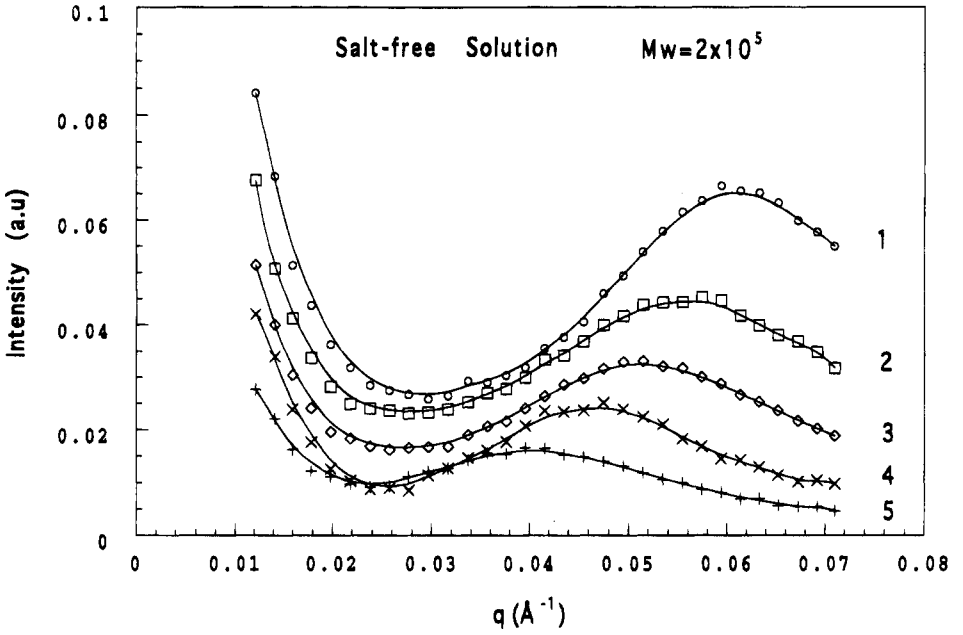

Figure 2. Effect of Concentration $I(q)$ versus q for salt-free solutions of xanthan at various polyelectrolyte concentrations C_p ($M_w = 2.0 \times 10^5$). Data labeled from 1 to 5 correspond to C_p = 30, 20, 15, 10, and 5 × 10^{-3} g/mL. The solid lines are guides to the eyes (T = 25 °C).

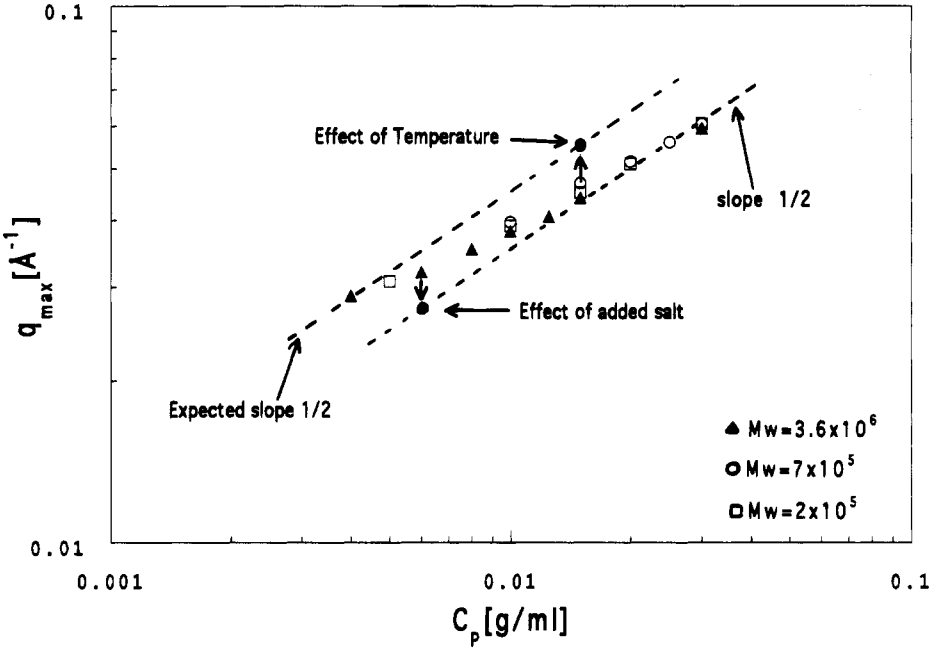

Figure 3. Variation of $\log[q_{max}]$ as a function of $\log[C_p]$ for the three studied molecular weights at T = 25 °C, in pure D_2O. The arrows (↑) show the influence of an increase in temperature and ionic salt concentration on the position of the peak. ● represents the limit of the shift at the highest temperatures and ionic salt concentrations used.

basis of semidilute to dilute behavior. Another process should be at the origin of the change of the exponent as the concentration decreases. In the light of Table 1, the conformational transition can be involved. Thus this change in the behavior, where the slope may take any value, represents, in our interpretation, a transition between two regimes having $C_p^{1/2}$ behavior for the two different conformations of xanthan. This interpretation is confirmed by the influence of the temperature and salt concentration on the peak position, as shown in Figure 3.

To go further in our analysis, the distance between chains (or segments) was calculated on the basis of the Bragg relation $D_{EXP} = 2\pi/q_{max}$. This distance decreases with increasing concentration, and the values are reported in Figure 4 (for instance, 4×10^{-3} g/mL < C_p < 3×10^{-2} g/mL for $M_w = 6 \times 10^6$). This behavior is in agreement with many experimental results reported for polyelectrolytes when using SANS,[14] SAXS,[12] and light-scattering[16-24] experiments.

To what does this distance correspond? In order to be more quantitative, we calculated the interparticle distance by assuming different conformations of the chain (or segment) in the semidilute regime: (i) D_{CU} assuming simple cubic distribution of the particle in solution; (ii) interparticle distance D_{LK}, calculated using the Lifson–Katchalsky model (in this case, the solution is divided into cylindrical subvolumes, parallel to each other, whose axis corresponds to the locally stretched polyelectrolyte; in this model the distance between

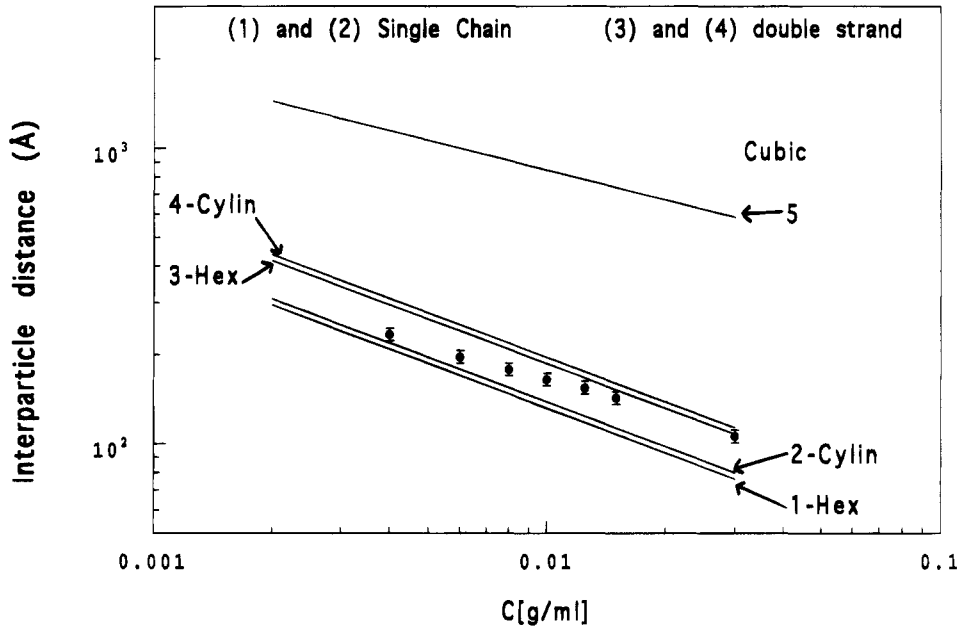

Figure 4. Comparison between experimental data (●) and theoretical prediction of the interparticle distance D with polymer concentration for $M_w = 3.6 \times 10^6$. Straight lines 1 and 2 correspond respectively to hexagonal and cylindrical packing of the single chain. Those corresponding to a double-stranded chain correspond to 3 (hexagonal), 4 (cylindrical), and 5 (simple cubic).

chains is independent of the molecular weight of the polymer); (iii) D_{HE} assuming hexagonal packing of stretched rodlike particles.

On the basis of this comparison, it is definitively clear that a simple cubic distribution cannot be at the origin of this interparticle distance since D_{CU} depends on the molecular weight and the disagreement becomes more and more pronounced ($D_{CU} >> D_{EXP}$) as the molecular weight and the concentration increase (see Figure 4, curve 5).

For the lowest concentrations, i.e. $C_p < 4 \times 10^{-3}$ g/mL, corresponding to the beginning of a second domain where q_{max} is expected to scale with C_p as $C_p^{1/2}$ the interparticle distance values are close to those calculated by assuming the Lifson–Kachalsky model. As the concentration increases, this agreement becomes less and less satisfactory due to the conformational transition (see Table 1). But at concentrations higher than $C_p \sim 12.5 \times 10^{-3}$ g/mL the semidilute features are recovered with a scaling law $q_{max} \sim C_p^{1/2}$. In this range of concentration a single chain (segment) distribution cannot explain the interparticle distance. However, if one assumes a withdrawal of the chain (segment) or a dimerization, one finds a good agreement with a hexagonal packing of fully stretched rodlike electrostatic segments. This behavior is illustrated in Figure 4. Straight lines 1 and 2 correspond respectively to hexagonal and cylindrical packing of a single chain. Those corresponding to a double-stranded chain correspond to 3 (hexagonal) and 4 (cylindrical).

These results are in agreement with the existence of a transition from ordered (3 or 4) to disordered state (1 or 2) of the chain as the concentration decreases (Table 1). At concentrations $C_p < 2 \times 10^{-3}$ g/mL and $C_p > 12 \times 10^{-3}$ g/mL, the system presents all the semidilute polyelectrolyte features. Namely, a scaling law $q_{max} \sim C_p^{1/2}$ and a rodlike packing behavior of a single chain at $C_p < 2 \times 10^{-3}$ g/mL and a withdrawal of the chain (segment) or a dimerization at $Cp > 12 \times 10^{-3}$ g/mL in a hexagonal or cylindrical packing within experimental errors.

Between these two domains of concentration a conformational transition exists (Table 1). This transition depends on the added salt concentration and on the temperature. The salt effect has been already presented in the ordered conformation ($C_p = 15 \times 10^{-3}$ g/mL) to show the electrostatic nature of the peak, and the next section discusses the temperature and salt effects on the basis of conformational transition.

III.3. Effect of Salt and Temperature. Depending on the range of concentration in the case of xanthan, the position and the height of the peak may be sensitive or not to added salt and/or temperature change in relation to the conformational transition. In fact, at concentrations above the crossover, in the ordered conformation and where $q_{max} \sim C_p^{1/2}$, there should be no effect of added salt on the position of the peak; the ordered conformation is stabilized. This has been already discussed in section 1. Nevertheless, at $C_p = 6 \times 10^{-3}$ g/mL when xanthan is under the disordered conformation at 25 °C,[35] a salt addition stabilizes the ordered conformation and then q_{max} decreases to the straight line which characterizes this conformation (see Figure 3).

As far as the temperature effect is concerned, our results yield to the following observations. At any concentration above 4×10^{-3} g/mL in pure D_2O the shape and the position of the peak of $I(q)$ versus q are very sensitive to the temperature (over the range 20–80 °C). This behavior is illustrated in Figure 5a for a xanthan solution having molecular weight $M = 3.6 \times 10^6$ and $C_p = 15 \times 10^{-3}$ g/mL. There is a broadening and decrease in peak intensity with increasing temperature. Moreover the peak position is shifted toward higher q values as the temperature increases. Figure 5b illustrates this behavior where the peak position and the intensity at the maximum are plotted as a function of temperature. One observes a clear transition around $T = 50$ °C. The broadening and the decrease in peak height are a consequence of thermal motion between scatterers and may be also a consequence of the decrease in the charge parameter in the disordered conformation as compared to the dimer state. According

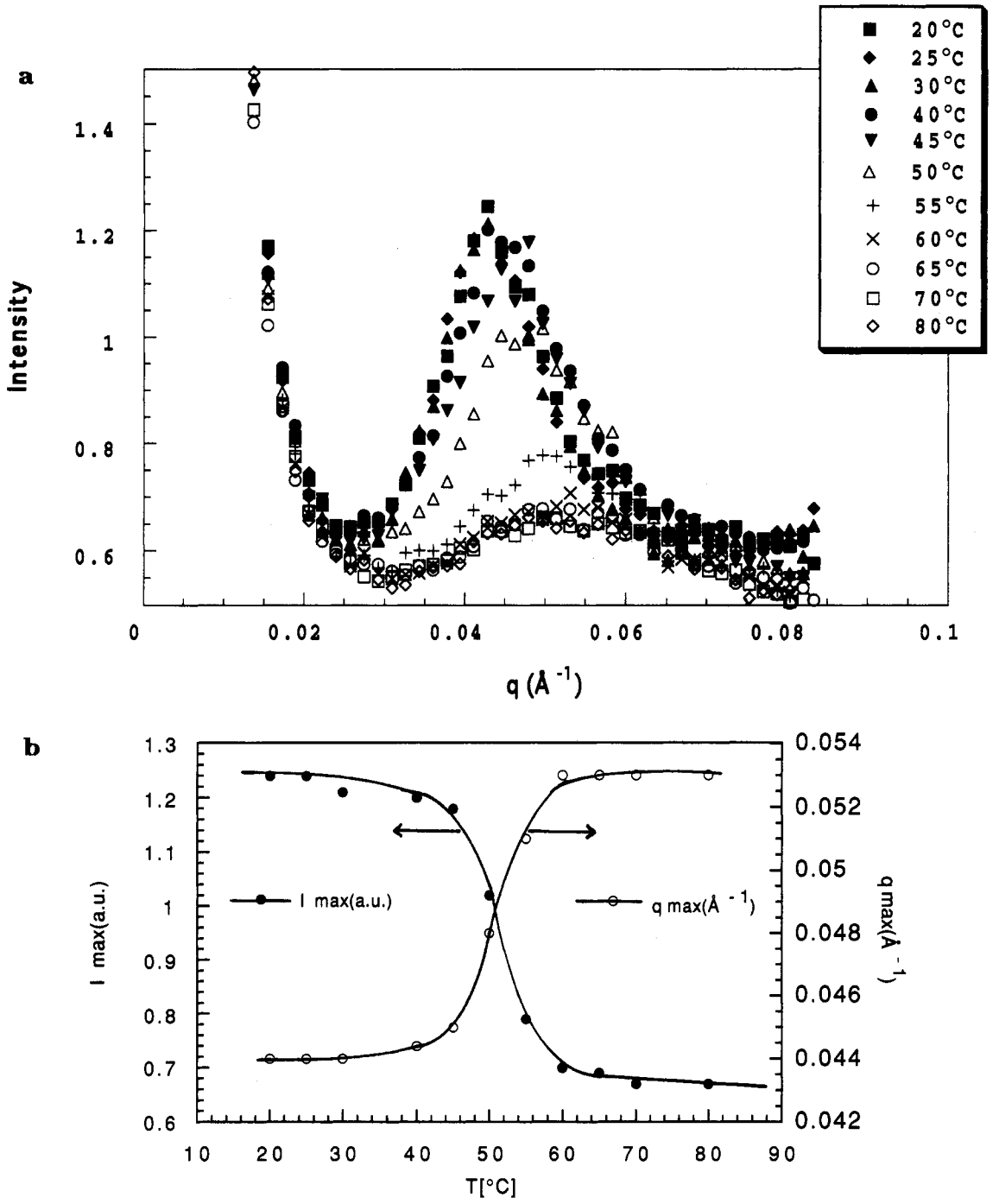

Figure 5. (a) $I(q)$ versus q for salt-free solutions of xanthan at $C_p = 15 \times 10^{-3}$ g/mL for various temperatures. (b) Variation of $I(q)_{max}$ and q_{max} versus temperature for a salt-free solution of xanthan at polyelectrolyte concentration $C_p = 15 \times 10^{-3}$ g/mL.

to Figure 6, the value of the melting temperature and the domain of temperature of the conformational transition determined by optical rotation is the same as that found for the q_{max} vs T variation. Then the change in the peak position with the temperature is a consequence of conformational transition. One notes that the q_{max} value at the highest temperature takes an expected value corresponding to a disordered single xanthan chain. Knowing that this transition takes place without molecular weight change[34,35] favors the folding of the xanthan chain as a description of the ordered conformation, at least for high molecular weights. This assumption is strengthened by the results of electron microscopy[37] and steric exclusion chromatography.[38]

IV. Conclusion

In this paper we have investigated the structure of xanthan solutions in the semidilute range of concentrations with and without added salt concentration using SANS. The results show the existence of a single, pronounced peak, in the scattered intensity which is lost with the addition of salt. The peak position remains unchanged for different M_w and ionic concentrations where the ordered conformation of the xanthan is established. The simplest explanation consistent with all the observations is interpreted in terms of strong repulsive interactions between nearest chains or segments at the intermolecular level. A scaling law, $q_{max} \sim C_p^{1/2}$, already predicted[4] and observed[14,39] is again confirmed in our observation. The new result is the

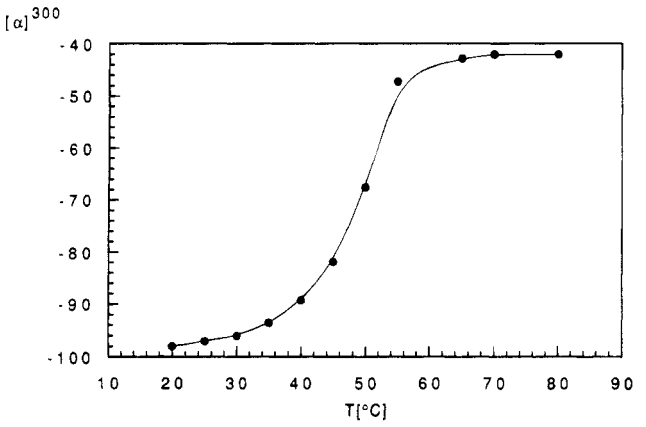

Figure 6. Optical rotation versus temperature for xanthan at 15×10^{-3} g/mL in pure D_2O (values taken by decreasing temperature to avoid disturbance by mesophase formation).

correlation of the peak position with the conformational transition of xanthan. When the xanthan undergoes a conformational change, induced by either a change in temperature or in xanthan or salt concentration, as described in this work, a displacement of the peak is observed. The peak position is shifted at lower q values during the transition (observed by other techniques[35]) from the disordered to the ordered state. Above the crossover, the xanthan conformation is ordered and the peak position becomes independent of the salt concentration. The corresponding interparticle distance is found to be in good agreement with a hexagonal packing by assuming a double-stranded xanthan form at least locally. When the temperature is increased above the melting temperature of the ordered conformation, the hexagonal packing is recovered involving single chains, as obtained in diluted solution $C < 4 \times 10^{-3}$ g/mL. Then, the results lend strength to the notion that the ordered conformation has roughly a double mass per unit length compared to the disordered xanthan conformation. The independence of the peak position from the molecular weight is in agreement with the hexagonal model.

In addition to this peak and in both conformations, there is a distinct upturn of scattered intensity as usually observed[14] in the very small q range (typically, $q < 0.02$ Å^{-1}) for all studied samples. At this stage we just mention this point without going further in our analysis. So far the origin of this upturn is not yet solved and no definitive explanation or interpretation has been accepted by the scientific community.

References and Notes

(1) Katchalsky, A.; Alexandrowicz, Z.; Kedem, O. In *Chemical Physics of Ionic Solutions*; Conway and Barradas, Eds; Wiley: New York, 1976.
(2) De Gennes, P. G. *Scaling Concepts in Polymer Physics*; Cornell University Press: Ithaca, NY, 1979; pp 64, 65.
(3) Hayter, J.; Jannink, G.; Brochard, F.; de Gennes, P. G. *J. Phys. Lett. (Paris)* **1980**, *41*, L-451.
(4) De Gennes, P. G.; Pincus, P.; Velasco, R. M.; Brochard, F. *J. Phys. (Paris)* **1976**, *37*, 1461.
(5) Benmouna, M.; Weill, G.; Benoit, H.; Akcasu, A. Z. *J. Phys. (Paris)* **1982**, *43*, 1679.
(6) Odijk, T. *J. Polym. Sci., Polym. Phys. Ed.* **1977**, *15*, 477.
(7) Skolnick, J.; Fixman, M. *Macromolecules* **1977**, *10*, 9444.
(8) Le Bret, M. *J. Chem. Phys.* **1982**, *76*, 6273.
(9) Manning, G. S. *Q. Rev. Biophys.* **1978**, *11*, 179.
(10) Hess, W.; Klein, R. *Adv. Polym. Sci.* **1982**, *32*, 173.
(11) Vilgis, T. A.; Borsali, R. *Phys. Rev.* **1991**, *A43*, 6857.
(12) Ise, N. *Angew. Chem., Int. Ed. Engl.* **1986**, *25*, 323.
(13) Kaji, K.; Urakawa, H.; Kanaya, T.; Kitamaru, R. *J. Phys. (Paris)* **1988**, *49*, 993.
(14) Nierlich, M.; et al. *J. Phys. (Paris)* **1979**, *40*, 701.
(15) Plestil, J.; et al. *Polymer* **1986**, *27*, 839.
(16) Drifford, M.; Dalbiez, J. P. *J. Phys. Chem.* **1984**, *88*, 5368.
(17) Xiao, L.; Reed, W. F. *J. Chem. Phys.* **1991**, *94*, 4568.
(18) Ghosh, S.; Peitzsch, R. M.; Reed, W. F. *Biopolymers* **1992**, *32*, 1105.
(19) Lin, S. C.; Li, W. I.; Schurr, M. *J. Biopolym.* **1978**, *17*, 1041.
(20) Sedlak, M.; Amis, E. J. *J. Chem. Phys.* **1992**, *96*, 817.
(21) Morfin, I.; Reed, W.; Rinaudo, M.; Borsali, R. *J. Phys. II* **1994**, *4*, 1001.
(22) Forster, S.; Schmidt, M.; Antonietti, M. *Polymer* **1990**, *31*, 781.
(23) Maier, E. E.; Krause, R.; Deggelmann, M.; Hagenbtchle, M.; Weber, R.; Fraden, S. *Macromolecules* **1992**, *25*, 1125.
(24) Schmitz, K. *Dynamic Light Scattering by Macromolecules*; Academic Press: New York, 1990; Chapter 10.
(25) Holzwarth, G. *Biochemistry* **1976**, *15*, 4333.
(26) Morris, E. R.; Rees, D. A.; Young, G.; Walkinshaw, M. D.; Dark, A. *J. Mol. Biol.* **1977**, *110*, 1.
(27) Paoletti, S.; Cesaro, A.; Delben, F. *Carbohydr. Res.* **1983**, *123*, 173.
(28) Milas, M.; Rinaudo, M. *ACS Symp. Ser.* **1981**, *150*, 25–30.
(29) Dentini, M.; Crescenzi, V.; Blasi, D. *Int. J. Biol. Macromol.* **1984**, *6*, 93.
(30) Paradossi, G.; Brant, D. A. *Macromolecules* **1982**, *15*, 874.
(31) Tinland, B.; Rinaudo, M. *Macromolecules* **1989**, *22*, 1863.
(32) Bezemer, L.; Ubbink, J. B.; de Kooker, J. A.; Kuil, M. E.; Leyte, J. C. *Macromolecules* **1993**, *26*, 6436.
(33) Maret, G.; Milas, M.; Rinaudo, M. *Polym. Bull.* **1981**, *4*, 291.
(34) Milas, M.; Rinaudo, M. *Carbohydr. Res.* **1986**, *158*, 191.
(35) Milas, M.; Rinaudo, M. *Carbohydr. Res.* **1979**, *76*, 189.
(36) Rinaudo, M.; Milas, M.; Jouon, N.; Borsali, R. *Polymer* **1993**, *34*, 3710.
(37) Stokke, B. T.; Smidsrod, O.; Elgsaeter, A. *Biopolymers* **1989**, *28*, 617–637.
(38) Milas, M.; Reed, W.; Printz, S. *Int. J. Polym. Anal. Characterization*, in press.
(39) Rinaudo, M.; Milas, M.; Duplessix, R. *Annu. Rep. ILL* **1982**, ILL experiment No. 9-11-14.

MA946096X